Simultaneous optimization of the design and operation of multi-generation energy systems based on life cycle energy and economic assessment

Simultaneous optimization of the design and operation of multi-generation energy systems based on life cycle energy and economic assessment

Hilal Bahlawan[a], Mirko Morini[b], Michele Pinelli[a], Pier Ruggero Spina[a], Mauro Venturini[a]

[a] *Dipartimento di Ingegneria, Università degli Studi di Ferrara, Via Saragat, 1, 44122 Ferrara, Italy*
[b] *Dipartimento di Ingegneria e Architettura, Università degli Studi di Parma, Parco Area delle Scienze 181/a, 43124 Parma, Italy*

Abstract

Multi-generation energy systems could mitigate global energy consumption, carbon emissions and economic costs. The promising energy, environmental and economic advantages of these systems are greatly dependent on their design and operational strategy. Consequently, methods and guidelines for the optimal design and operation of such systems, also taking into consideration their life cycle, are needed to fully exploit their potential. This paper proposes a general methodology for the simultaneous optimization of the design and operation of multi-generation energy systems by considering life cycle energy and economic assessment. The design optimization problem is solved by means of surrogate modeling and the operation optimization problem by means of dynamic programming. The multi-generation energy system considered in this paper comprises renewable energy systems, fossil fuel energy systems and energy storage technologies. Different multi-objective optimizations were performed by considering the minimization of fossil cumulative energy demand, and total investment and operational costs. The validity of the proposed methodology is demonstrated by using the campus of the University of Parma (Italy) as a case study. Compared to a conventional plant, the optimal solution allows a life cycle energy saving of about 17% and total cost reduction of about 18%. Moreover, compared to an optimization method based on particle swarm optimization and dynamic programming, the proposed methodology provides comparable results, but the computation time is 78% lower. The proposed methodology outperforms commonly used optimization algorithms and provides an effective and flexible framework for the optimal design and operation of multi-generation energy systems.

Keywords: Design optimization; Life cycle assessment; Multi-generation energy systems; Operation optimization.

Nomenclature

Abbreviations

AC	absorption chiller
ASHP	air source heat pump
CC	compression chiller
CHP	combined heat and power
COP	coefficient of performance
CP	conventional plant
DP	dynamic programming
EER	energy efficiency ratio
FCED	fossil cumulative energy demand
GA	genetic algorithm
GB	gas boiler
IC	investment cost
ISO	international organization for standardization
LCA	life cycle assessment
LCI	life cycle inventory
LCIA	life cycle impact assessment
MES	multi-generation energy system
MILP	mixed integer linear programming
OF	objective function
PV	photovoltaic system
SMO	surrogate modeling optimization
STC	solar thermal collector
TC	total cost
TES	thermal energy storage
TOC	total operational cost

Symbols

A	area
c	dissipation coefficient
d	sample
E	energy
G	solar irradiance
h	intermediate cost function
l	generic energy system

m	mass
N	time period
P	power
q	polynomial
s	interpolation function
T	temperature
u	control variable
V	volume
W	weight
x	state variable
Z	cost function
α	weight of the energy objective
λ	number
Φ	radial basis function
β	weight of the economic objective
δ	share of material flow
η	efficiency

Subscripts and superscripts

Al	allocation
amm	amortized
BoS	balance of system
cool	cooling
D	dimension
diss	dissipation
el	electrical
f	material flow
GN	gas network
grid	national grid
i	generic material flow
in	entering
int	interest rate
k	time variable
M	module
n	number of samples
nom	nominal
out	outgoing
op	optimal
p	amortization period
ref	reference
sent	sent to the grid
taken	taken from the grid
th	thermal
tot	total

1. Introduction

1.1 Problem statement and literature review

Global primary energy consumption is expected to grow exponentially over the next few years due to the increase in energy demands for heating, cooling and lighting [1]. For instance, buildings are responsible for about 32% of global final energy consumption and 30% of global greenhouse gas emissions [2]. Multi-generation energy systems (MESs) [3] have emerged as one of the most effective solutions for the reduction of energy consumption, energy costs and CO_2 emissions of buildings, universities, districts, and communities [4]. However, the promising energy, environmental and economic advantages of these systems are greatly dependent on their design and operational strategy. Consequently, methods and guidelines for the optimal design and operation of such systems, also taking account of their life cycle, are needed to fully exploit their potential.

Compared to separate energy production by means of conventional plants, MESs could mitigate the crisis of carbon emissions and achieve sustainable development by combining several energy technologies fed by renewable and fossil energy sources in a unique energy system, to supply heating, cooling and electrical energy [5]. Indeed, the proximity of MESs to the end-users reduces energy transmission losses and increases energy efficiency. Furthermore, the integration of multiple energy technologies, such as combined heat and power (CHP) systems, heat pumps, absorption chillers (ACs) and energy storage technologies, allows heating, cooling and electricity to be combined with the benefits of initiating new business opportunities [4]. Hassoun et al. [6] investigated a MES comprising a photovoltaic (PV) panel, wind turbine, diesel generator and battery bank system for power, freshwater, and cooling. The energy and exergy analyses of the system showed that an exergy efficiency equal to 49% may be achieved. Khalid et al. [7] presented a solar-biomass plant composed of a concentrated solar collector, organic Rankine cycle, gas turbine and AC to supply space heating, cooling, power and hot water. They found that the proposed system is more efficient and more cost-effective than using individual solar and biomass energy systems. Chitgar et al. [8] proposed a novel MES based on a solid oxide fuel cell integrated with a Kalina cycle, thermoelectric generator, and reverse osmosis desalination for power and freshwater production. The results showed that the energy and exergy efficiencies increase as the pressure in the Kalina turbine increases. A solar-based MES for greenhouse application has been analyzed by Mahmood et al. [9]. The thermodynamic analysis revealed that solar radiation may significantly affect the overall performance of the system.

The energy and economic performance of MESs are greatly dependent on their design and operational strategy. Therefore, implementing methods for design and operation optimization is a key factor to achieve the expected benefits from MESs with minimal energy consumption and economic costs [10]. The presence of several energy technologies in a single plant that supplies energy to one or multiple users, the use of different sources of energy, and the connection to different energy networks make the optimization of MESs a very complex task. Several methods have been presented in the literature to identify the integrated optimal design and operation of MESs [11]. Fakhari et al. [12] optimized the operating conditions of a novel biomass-based MES comprising a gasification unit, a fuel cell, a multi-effect desalination unit, and a series two-stage organic Rankine cycle using various zeotropic mixtures for the use of waste heat for heat, power, and freshwater production. The multi-objective optimization results revealed that, at best, the exergy efficiency is 23.43%, the produced freshwater is 162.86 m^3/day, and the total cost rate equals 64.91 $/h. Furthermore, a hydrogen-based fuel cell integrated with an organic Rankine cycle with zeotropic mixtures has been also investigated by the same authors in [13]. The system has been optimized by using a genetic algorithm (GA) and performing multi-objective optimizations. The results of the multi-objective optimization showed that it is more efficient to use a low-temperature fuel cell than a high-temperature fuel cell. Urbanucci et al. [14] presented an optimization procedure for the integrated design and operation optimization of CHP systems. They defined the operation strategy of the systems by using rule-based methods and they did not consider the option of integrating renewable energy systems. A more complex system composed of a CHP, PV, wind turbine and battery storage was considered in [15]. The study aimed to find the optimal sizes of the system components by using a Grey Wolf optimization algorithm, while the operational strategy of the system components was defined by a rule-based energy management strategy. The design problem of a hybrid renewable energy system composed of PV, wind turbine, diesel generator and battery storage technologies was addressed in [16]. The design variables were optimized by using the software Homer Pro®, while the traditional electrical load following strategy was used to control the different systems. Alirahmi et al. [17] proposed and optimized the design variables of a multi-generation system using an evolutionary algorithm to maximize the exergy efficiency and minimize the cost rate. Vojdani et al. [18] implemented multi-objective optimizations to determine the best operating conditions of an integrated energy system comprising a solid oxide fuel cell, gas turbine and multi-effect desalination unit for power and freshwater production. The optimization was performed by considering the exergy efficiency, production cost and environmental impact as objectives. The results showed that the exergy efficiency of the optimal solution is 69.70%, the production cost is 29.33 $/MWh, while the environmental impact is 299.23 kgCO2/MWh.

Even though the works mentioned above add a significant contribution to the literature, none of them considers the simultaneous optimization of the design and operational strategy of the employed technologies. Indeed, these two issues are deeply interrelated and must be addressed simultaneously because the definition itself of an optimal operation strategy strongly depends on the optimal design of the energy plant and vice versa. This problem has been addressed by Evins et al. [19] who investigated the design and operation optimization problem of an energy plant and presented a multi-level optimization approach based on a GA and mixed-integer linear programming (MILP). The plant design and operational variables were optimized by minimizing capital costs, running costs and carbon emissions. Fonseca et al. [20] presented a multi-criteria optimization method for the design and operation of distributed energy plants. The results showed that, compared to a decentralized scenario, emissions can be reduced up to 89%. However, the optimization was performed by considering a time step of 12 h and ignoring the intraday variation of solar radiation. A two-phase collaborative optimization method has been proposed by Liu et al. [21] to determine the optimal design of a distributed energy system. The optimal sizes of the different systems considered in the plant have been determined under different operation strategies and by minimizing primary energy consumption and annual costs. The optimization results showed that the proposed system is reliable and feasible in providing a nearly zero-energy community with various energy sources. Luo et al. [22] presented a two-stage optimization approach to simultaneously optimize the capacities and operation of a MES by using a GA. To reduce computational time, the optimization problem has been solved by considering the winter week and summer week with the highest heating and cooling load, respectively. Compared to the capacity optimization following electricity load, the proposed approach can reduce the year-round biomass consumption by about 14%. Moreover, Piacentino et al. [23] proposed a MILP model for the design and operation optimization of tri-generation systems to minimize the net present cost. Similarly, the design and operation optimization problem of a MES with high renewable penetration has been solved by Zhang et al. [24]. They linearized the constraints and solved the problem as a MILP showing that the model proposed is suitable for the design and planning of MESs. Furthermore, Urbanucci et al. [25] presented a methodology for the simultaneous design and operation optimization of CHP systems with thermal energy storage (TES) and auxiliary boiler. The design problem was solved using GA, while the operation is optimized by using a MILP. To overcome the challenge of computational complexity, the authors decomposed the original optimization period of one year into several sub-periods. Despite the effectiveness of MILP-based methods in solving the design and operation optimization of energy plants, they are only suitable for linear problems [26]. Yet, the general problem of the simultaneous design and operation optimization of MESs usually results in a non-linear problem. Moreover, complex systems require a very large computation time due to the very large number of decision variables [27]. Therefore, to use MILP methods, assumptions have to be made to achieve the linearity of the problem and reduce the computational complexity.

The long-running time is one of the major obstacles to energy system optimization. Among the various optimization methods proposed in the literature, several researchers have focused on the implementation of surrogate models or meta-models to overcome the computational complexity of expensive objective functions. The basic idea of the surrogate modeling approach is to approximate the original computationally expensive objective function through tractable functions, which have well-known properties, such as the radial basis function [28]. Zhang et al. [29] used a surrogate model to find out the influencing factors of a hybrid battery thermal management system for electric vehicles, such as heat dissipation performance, and performed multi-objective optimization to determine the optimal design parameters. The results showed that the optimized system can dissipate heat and maintain temperature uniformity. Likewise, Beykal et al. [30] implemented surrogate models for multi-objective optimization of an energy market design problem. The proposed method outperformed other available algorithms. Perera et al. [31] developed a surrogate model by using neural networks to optimize both design and dispatch strategy of an energy plant composed of wind turbines, PV, a battery bank and an internal combustion generator. The proposed algorithm is able to reduce the computational time by up to 84%. In addition to surrogate modeling, dynamic programming (DP) has also recently attracted lots of research in the area of energy system optimization due to its ability to deal with non-linear optimization problems and identify globally optimal solutions in the discrete state space [32]. The DP method is mainly used to optimize the operational strategy of energy systems where the behavior of the plant is described by means of state variables [33]. In our recent study [34], we found that the operation strategies defined by DP always outperform commonly used operation strategies. The application of DP to solve energy management problems has also been addressed by several studies. For instance, Facci et al. [35] presented a methodology to determine the optimal operation strategy of a tri-generation plant based on fuel cell technology. They applied the DP method by considering the energy and economic objective functions and the hourly electrical, thermal and cooling energy demands for a small hotel. The optimized control strategy allowed a reduction in the primary energy consumption and operational costs of the plant. Moradi et al. [36] demonstrated the effectiveness of a DP optimization method for the energy management of multi-source microgrids. They examined two operational scenarios that differ in the possibility of accessing battery storage, concluding that access to the battery may allow a further reduction in system cost and produced emissions.

When integrating renewable energy systems in MESs, optimization must also be performed by considering the entire life cycle of these systems and not only their useful life [37]. In fact, it is generally considered that the energy consumption and emissions of renewable energy systems amount to zero. However, there is considerable energy consumption and environmental emissions during their manufacturing and disposal. Multiple studies have addressed the design optimization of energy systems from a life cycle perspective. A renewable MES composed of a PV, solar thermal collector (STC), biomass CHP and AC was optimized in [38]. Life cycle primary energy consumption, economic cost and carbon emissions were considered as objectives. A linear scaling approach to evaluate the effect of the rated capacities of the system on the life cycle performance of the plant has been followed. Yan et al. [39] evaluated the environmental and economic impact of a system composed of micro-turbines, PVs and batteries by using an optimization method based on a parametric LCA framework. Compared to conventional power generation, the proposed system, which is operated by following the thermal load has less environmental impact. Mayer et al. [40] proposed an optimization method based on a GA for the design of a hybrid renewable energy plant considering the life cycle cost and environmental footprint. Due to the scarcity of data, they extrapolated the inventory data linearly with capacities of the plant components. The study demonstrated the relevance of life cycle assessment (LCA) in the design of hybrid renewable energy systems and the superiority of renewables to fossil fuels from an environmental point of view.

With the support of optimization methods, among different options, designers can effectively select the energy system configuration that has the best energy, cost and environmental performance from the viewpoint of its life cycle. The technical specifications and limitations of each system integrated in the plant have to be modeled with an appropriate level of details without compromising the computational complexity. Moreover, the life cycle inventory (LCI) data for each system need to be available in a range of sizes because energy technologies could vary in size and thus experience scale effects [41].

1.2 Contribution of this paper

This paper tackles an all-embracing challenge. In fact, despite the number of studies already published about the design of MESs, to the authors' knowledge, very few studies have been published on the simultaneous design and operation optimization of MESs. In particular, this is the first attempt to combine surrogate modeling and DP for energy system optimization. The MES considered in this paper comprises STC, PV, CHP, air source heat pump (ASHP), gas boiler (GB), AC, compression chiller (CC) and TES, since they are widely used to meet the thermal, cooling and electrical energy demands. A case study consisting of a University Campus is considered to demonstrate the validity of the proposed methodology. The design and operational strategy of the MES are optimized by considering the life cycle of fossil cumulative energy demand (FCED) and total costs (TCs) (i.e., investment and operational) in a single weighted-sum objective function. Compared to the studies available in the literature, the main contributions of this paper are as follows:

- a novel methodology combining surrogate modeling optimization (SMO) and DP is developed for the optimization of MESs. The proposed methodology is general and thus can be applied to any case study, such as buildings, universities and districts;
- instead of being limited to system design only, the design and operation problems, which are intrinsically related, are solved simultaneously. Moreover, the non-linear characteristics of the investigated energy technologies are also considered;
- multi-objective optimizations of a MES are performed to obtain the best design and operation strategy from a life cycle energy and economic perspective;
- the methodology provides design and operational results by considering one year of operation (instead of clustered days) in a reasonable computational time.

The paper is organized as follows: Section 2 presents the methodology, illustrates the energy plant, introduces the life cycle assessment of the considered energy systems, discusses the inventory scaling, and presents the impact indicators and economic assessment. Section 2 also highlights the optimization method. Section 3 outlines the case study. Section 4 discusses the results while the last section draws the conclusions.

2. Methodology

2.1 Multi-generation energy system modeling

As shown in Fig. 1, several types of energy systems fed by different energy sources are considered, namely a PV, STC, CHP system based on an internal combustion engine, ASHP, GB, AC, CC and TES. These technologies are suitable for applications as both single components and aggregate systems and are available on the market in a wide range of sizes (see Appendix A). Each system of the MES (including solar energy systems) is modeled by following a grey-box modeling approach. These steady-state models are defined by means of power and efficiency curves and are implemented in Matlab®. Moreover, in order to consider the seasonal efficiency variation of the different systems, the efficiency of all systems (except the GB and AC) is corrected as a function of the ambient temperature by following the approach reported in Barbieri et al. [42]. The simulation of the MES is performed throughout one year and the analysis is conducted on an hourly basis. For the sake of brevity, the system models are not reported in this paper. More details about these models have been described in our previous work [37].

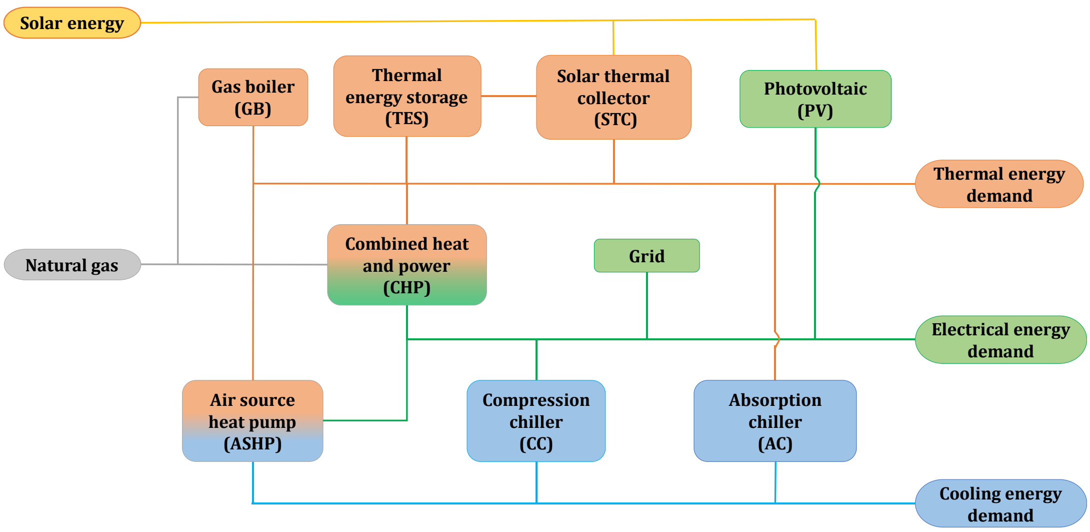

Fig. 1. Layout of the MES.

The optimal design and operation strategy of the MES is conducted by fulfilling user energy demands. Equations (1) through (6) represent the energy balance constraints and the energy flows of the energy systems included in the MES [42]. In particular, the user's thermal demand at time step k can be met by the STC, CHP, ASHP, GB and TES, the cooling demand can be met by the ASHP, AC and CC, while the user's electrical demand, the heat pump and the chiller are fulfilled by the PV, CHP and grid.

$$E_{\mathrm{user,th,k}}=E_{\mathrm{STC,th\rightarrow user,k}}+E_{\mathrm{CHP,th\rightarrow user,k}}+E_{\mathrm{ASHP,th,k}}+E_{\mathrm{GB,th\rightarrow user,k}}+E_{\mathrm{TES,th,out\rightarrow user,k}} \tag{1}$$

$$E_{\mathrm{user,cool,k}}=E_{\mathrm{ASHP,cool,k}}+E_{\mathrm{AC,cool,k}}+E_{\mathrm{CC,cool,k}} \tag{2}$$

$$E_{\mathrm{user,el,k}}+E_{\mathrm{ASHP,el,k}}+E_{\mathrm{CC,el,k}}=E_{\mathrm{PV,el,k}}+E_{\mathrm{CHP,el,k}}+E_{\mathrm{grid,el,taken,k}} \tag{3}$$

$$E_{\mathrm{CHP,th,k}}=E_{\mathrm{CHP,th\rightarrow user,k}}+E_{\mathrm{CHP,th\rightarrow AC,k}}+E_{\mathrm{CHP,th\rightarrow TES,k}} \tag{4}$$

$$E_{\mathrm{STC,th,k}}=E_{\mathrm{STC,th\rightarrow user,k}}+E_{\mathrm{STC,th\rightarrow AC,k}}+E_{\mathrm{STC,th\rightarrow TES,k}} \tag{5}$$

$$E_{\mathrm{AC,th,in,k}}=E_{\mathrm{STC,th\rightarrow AC,k}}+E_{\mathrm{CHP,th\rightarrow AC,k}}+E_{\mathrm{TES,th\rightarrow AC,k}}+E_{\mathrm{GB,th\rightarrow AC,k}} \tag{6}$$

2.2 Life cycle assessment

The energy and environmental performance of products is one of the concerns of today's world. LCA is a methodology that evaluates energy consumption, environmental impact and the resources used by analyzing all stages of the product life cycle, i.e., from raw material extraction, via production and use phases, to end-of-life. LCA helps to compare different products with the same functional unit and to select the product that has the least energy and environmental impact. The International Organization for Standardization (ISO) developed global technical standards for LCA, i.e., ISO 14040 [43] and ISO 14044 [44]. The LCA process is a systematic approach that includes four separate phases: Goal and scope definition, Inventory analysis, Impact assessment and Results interpretation.

2.2.1 Goal and scope definition

Goal definition is the phase of LCA that defines the purpose of the study. In this study, the purpose is the quantification of the FCED through a cradle-to-gate LCA for various types of energy systems in a range of sizes. The LCA results are useful for MES design optimization that includes different energy technologies with different sizes. Moreover, they are helpful for designers as a decision support to easily assess whether or not an option is favorable in terms of energy consumption and the environmental impact.

The functional unit of CHP, GB, ASHP, CC and AC is defined by the respective nominal power (i.e., thermal, cooling or electrical power). Instead, the functional unit of PV and TES is represented by the corresponding area and volume, respectively. This choice of the functional unit is helpful to assess the FCED of the systems in a range of sizes.

As shown in Fig. 2, the impact related to the production of the investigated technologies is assessed by means of a cradle-to-gate LCA approach. The dismantling phase of the considered systems is ignored in this paper because no consolidated information is available. Thus, as highlighted in Fig. 2, the LCA study carried out in this paper includes raw material extraction and the processing, transportation and manufacturing of the final system. The energy consumption during the use phase is quantified by considering a case study (Section 3).

Since the LCA study is conducted on market available energy systems with a focus on the European market, standard distances of 100 km in lorry and 200 km in freight train are assumed [45] for the manufacturing of the different systems. Moreover, the schemes of the European energy and electricity mix are adopted for the evaluation of the demanded energy and electricity.

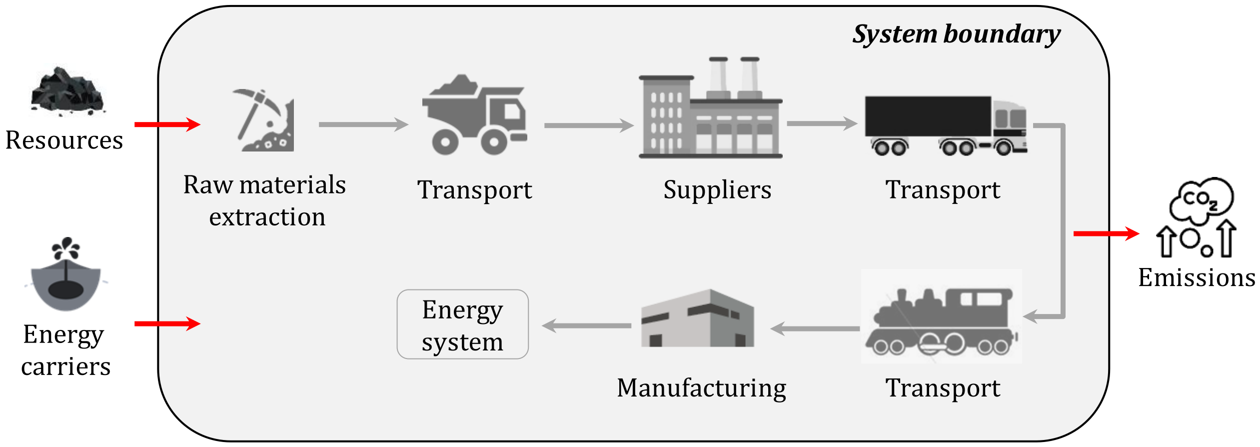

Fig. 2. Boundaries of the investigated energy system.

2.2.2 Inventory analysis and scaling

LCI consists of creating an inventory of input and output flows according to the system boundary defined at the goal and scope phase. The inventory flows include inputs of water, energy, raw materials and emissions to air, soil and water.

Figure 3 highlights the general procedure for the scaling of the LCI as a function of system size. By following the approach proposed by Caduff et al. [46], in a previous paper by the same authors [47], the scaling of the inventory of materials and energy use was made by considering the variation of the weight with system size, assuming that material composition (i.e., steel, aluminum, chromium, copper, etc.) is independent of system size. This was done because information about the dry weight of the system is usually available from the manufacturers, while data about material composition are rarely shared for confidentially reasons. Thus, the material composition of all systems was considered independent of size. Data about material composition and energy consumption for the manufacturing of the energy systems investigated were taken from the Ecoinvent 3.4 database [48] and the literature [49].

For each system, a market analysis was conducted and information about its weight was taken from the technical reports of the main manufacturers. The results of the market analysis, reported in [47], are summarized in Appendix A. As can be seen from Figs. A1 through A5, the relationship between the weight and the size of the system allows its scaling behavior (i.e., scaling laws) to be explored. Finally, given the scaling laws and material composition for each system, the inventory flows can be scaled at different sizes. In fact, the mass of each flow ($m_{f,i}$) of the inventory is determined by multiplying its share (δ_i) by the total weight (W) of the system. Once the inventory is scaled, an LCA model can be constructed and the impact can be assessed.

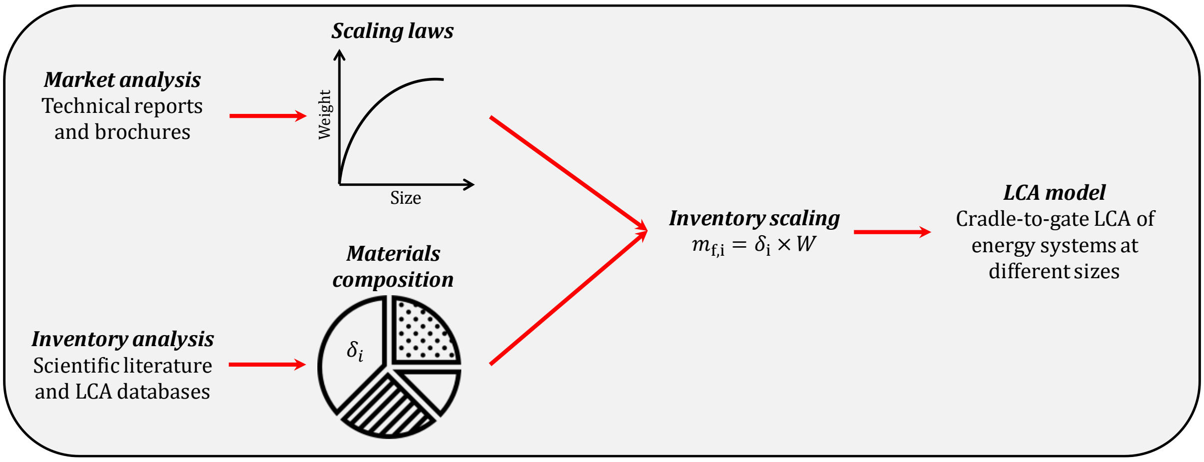

Fig. 3. Procedure for the inventory scaling of energy systems in a range of sizes.

2.2.3 Impact assessment

The life cycle impact assessment (LCIA) is the phase that establishes a link between the inventory of the elementary flows of a product and its potential environmental impact [50]. This evaluation is carried out by translating the elementary emissions from the inventory into environmental impact. Generally, the LCIA phase consists of the following three steps:

- Defining and selecting the impact category;
- Classifying and assigning the elementary flows to the respective impact categories;
- Characterizing and evaluating the environmental impact of each category.

In this paper, the considered impact is the FCED which is calculated by the method developed by the Ecoinvent center [51]. The LCA models of the investigated systems are implemented by using the software openLCA® 1.10.3 [52].

2.3 Economic assessment

As summarized in Table 1, the total investment cost (equipment and installation costs) is considered dependent on unit size. In particular, an economic assessment was preliminarily carried out by analyzing different sources with a focus on the European market and a scaling formula for the investment cost was obtained. The cost unit is expressed in € (Euro), which is the currency used in the European Union. The investment cost is calculated as a function of the installed area A for the STC and PV systems, as a function of the nominal electrical power $P_{el,nom}$

for the CHP, as a function of the nominal thermal power $P_{\text{th,nom}}$ for the ASHP and GB, as a function of the nominal cooling power $P_{\text{cool,nom}}$ for the AC and CC, and as a function of the maximum thermal capacity $E_{\text{th,max}}$ for the TES. Fixed and variable operational costs associated with the operation and maintenance of the energy systems are also considered. Regarding the PV, STC and TES, the fixed and operational costs are ignored because no moving parts are present in these systems. For instance, the operational costs for STC plants are lower than 1 €/MWh [53].

The fixed operational costs are expressed in [€/(kW·year)] and are independent of the running time of the system and how the system is operated. These costs include periodic operation and maintenance service, administration, insurance and operational staff. The variable costs are expressed in [€/kWh] and are calculated as a function of energy production. Fixed and variable operational costs do not include fuel and CO2 emission costs. The fuel and CO2 emission costs are accounted for separately, as reported in Section 3.

Table 1. Investment costs and fixed and variable operational costs for the different energy systems.

Technology	System size	Total investment costs [€]	Fixed costs [€/(kW·year)]	Variable costs [€/kWh]	Reference
STC	A [m^2]	$635.4 \times A^{0.869}$	-	-	[53-56]
PV	A [m^2]	$291 \times A$ (Residential scale) $239 \times A$ (Commercial scale) $172 \times A$ (Utility scale)	-	-	[57]
CHP	$P_{\text{el,nom}}$ [kW$_{\text{el}}$]	$2795.3 \times P_{\text{el,nom}}^{0.769}$	9	0.007	[53, 58, 59]
ASHP	$P_{\text{th,nom}}$ [kW$_{\text{th}}$]	$1049.6 \times P_{\text{th,nom}}^{0.946}$	3	0.0018	[53, 56, 58]
GB	$P_{\text{th,nom}}$ [kW$_{\text{th}}$]	$356.8 \times P_{\text{th,nom}}^{0.829}$	3	0.0005	[53, 55, 58, 60]
AC	$P_{\text{cool,nom}}$ [kW$_{\text{cool}}$]	$1684.7 \times P_{\text{cool,nom}}^{0.796}$	2	0.00028	[58, 61]
CC	$P_{\text{cool,nom}}$ [kW$_{\text{cool}}$]	$587.8 \times P_{\text{cool,nom}}^{0.946}$	3	0.0018	[53, 56, 58]
TES	$E_{\text{th,max}}$ [kWh]	$25 \times E_{\text{th,max}}$ ($E_{\text{th,max}} <= 3000$ kWh) $11 \times E_{\text{th,max}}$ ($E_{\text{th,max}} > 3000$ kWh)	-	-	[55, 58]

2.4 Optimization approach

Unlike the optimization methodologies exploited by the authors in previous works [10, 47], the optimization approach proposed in this paper combines design optimization (upper level) with operation optimization (lower level) in a single optimization problem that includes design and operational variables. Additionally, the optimization model is able to select the best combination of technologies that minimizes the objective function. The optimization is carried out by considering one full year and plant operation is simulated on an hourly basis.

The simultaneous optimization of the design and operational strategy addresses problems where the design optimization depends on the results of the operation optimization, which determines energy consumption and operational costs at each time-step, and consequently the total yearly energy consumption and economic costs. Moreover, the identification of the optimal operational strategy depends on the results of the design level, since this determines the available energy supplies of the different technologies.

The flowchart of the optimization approach proposed in this work is shown in Fig. 4. The design variables of the MES are optimized by using the SMO algorithm, while the operational variables are optimized by using the DP method.

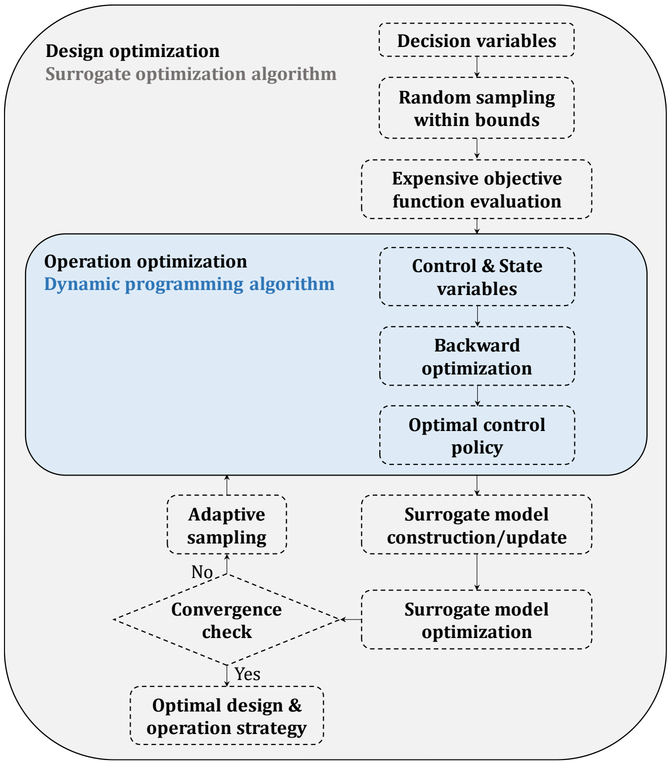

Fig. 4. Flowchart of the simultaneous design and operation optimization of the MES.

2.4.1 Design optimization

As outlined in Fig. 4, the design optimization problem is solved by means of a SMO algorithm. Generally, in surrogate-based optimization, a surrogate model is constructed to approximate a time-consuming objective function which may be discontinuous, non-differentiable and non-linear [62]. Surrogate-based optimization is of particular interest for the optimization of complex energy plants, where the optimization process would be computationally demanding, as in the case of MESs. Moreover, when considering the operational optimization problem, the computational complexity becomes higher and consequently, solving the design and operation optimization in one single step becomes very challenging. Therefore, an option to reduce the computational complexity is to build a surrogate model which emulates the behavior of the original model. As highlighted in Figs. 4 and 5, the optimization process starts by generating a set of samples $\{d_1, \dots, d_\mathrm{n}\} \in \mathbb{R}^\mathrm{D}$ in the design space, where n and D are the number of samples and dimension of the design space, respectively.

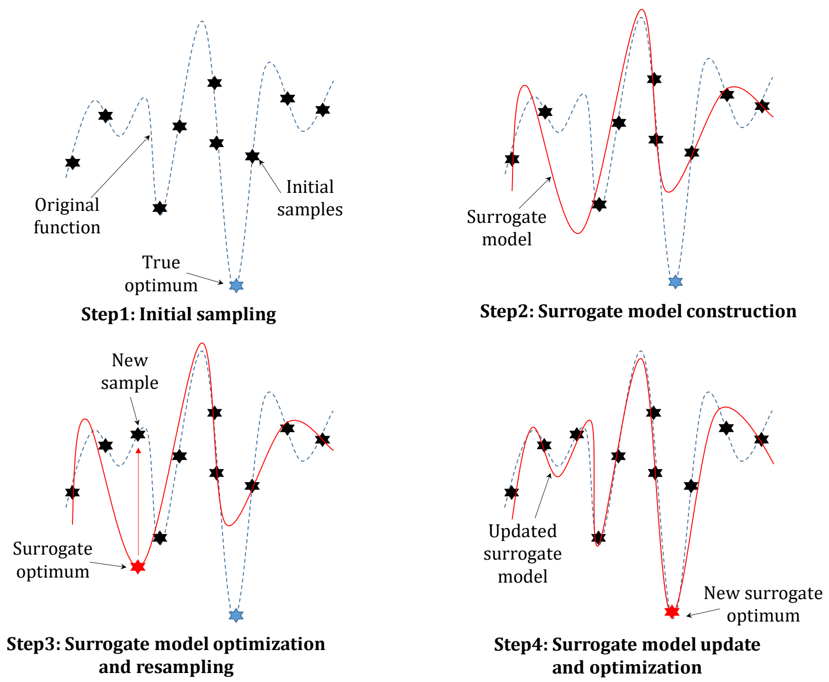

Fig. 5. Surrogate-based design optimization.

Once the expensive objective function values $\{\widehat{f}_1, \dots, \widehat{f}_{\mathrm{n}}\} \in \mathbb{R}$ at these points are evaluated, a surrogate model is constructed by interpolating a radial basis function. The interpolant can be represented as follows [63]:

$$s(d) = \sum_{\mathrm{i}=1}^{\mathrm{n}} \lambda_{\mathrm{i}} \times \Phi\left(\|d - d_{\mathrm{i}}\|\right) + q(d) \tag{7}$$

Where $s(d)$ interpolates the data $(d_1, \widehat{f}_1), \dots, (d_{\mathrm{n}}, \widehat{f}_{\mathrm{n}})$, $\lambda_i \in \mathbb{R}$ for $\mathrm{i} = 1, \dots, \mathrm{n}$, $\|\cdot\|$ is the Euclidean norm, $q(d)$ is a linear polynomial tail, and Φ denotes the radial basis function evaluated at the Euclidean distances. Different choices of radial basis functions are available, such as linear ($\Phi(r) = r$), cubic ($\Phi(r) = r^3$), and thin plate spline ($\Phi(r) = r^2 \times \log r$). In this study, cubic radial basis functions are used since they are simpler and work better than other forms, such as the thin plate spline [64]. Moreover, cubic radial basis functions are already implemented in the surrogate optimization solver of Matlab. As demonstrated by Powel et al. [65], constructing an interpolator based on radial basis functions involves solving an n-by-n linear system of equations (more details about the mathematical formulation of the problem can be found in Regis [64] and Powel [65]).

Once the initial surrogate model is optimized and their global solutions are found. The global solutions of the surrogate model are then used as new sampling points, the original problem is simulated at these points and the initial surrogate model is then updated using the new adaptive samples. Finally, this process is repeated until the best solution is found. As demonstrated in [63], the proposed algorithm was proven to converge to a global solution.

At design optimization level, the decision variables are defined as the optimal combination of systems among the considered candidates (i.e., STC, PV, CHP, ASHP, AC, GB, CC, TES) and the optimal sizes. Moreover, a decision variable (between 0 and 1) that defines the total available area for the PV and STC is also considered. The design optimization problem is solved by minimizing the following weighted sum objective function (OF) [26]:

$$OF_{\mathrm{SMO}} = \alpha \times \left(\frac{FCED}{FCED_{\mathrm{CP}}}\right) + \beta \times \left(\frac{TC}{TC_{\mathrm{CP}}}\right) \tag{8}$$

As reported in Eq. (8), the OF includes two potentially conflicting objectives, the $FCED$ and TC, both normalized to the case of a conventional plant (CP) composed of boilers, chillers, gas network and electric grid. Different scenarios are investigated by considering two weights, α and β, which assume values between 0 and 1.

Equation (9) represents the total $FCED$ calculated as follows [66]:

$$FCED = FCED_{\mathrm{MES}} + FCED_{\mathrm{grid}}\left(E_{\mathrm{grid,el,taken,year}}\right) + FCED_{\mathrm{GN}}\left(V_{\mathrm{fuel,CHP,year}}, V_{\mathrm{fuel,GB,year}}\right) - FCED_{\mathrm{CHP,AI}}\left(E_{\mathrm{CHP,el,sent,year}}\right) - FCED_{\mathrm{PV,AI}}\left(E_{\mathrm{PV,el,sent,year}}\right) \tag{9}$$

where;

$$FCED_{\mathrm{MES}} = \sum_{\mathrm{l}=1}^{\mathrm{S}} \frac{FCED_{\mathrm{l}}}{\mathrm{lifetime}_{\mathrm{l}}} \tag{10}$$

$$FCED_{\mathrm{CHP,Al}} = \eta_{\mathrm{CHP,el,avg,year}} \times \frac{E_{\mathrm{CHP,el,sent,year}}}{E_{\mathrm{CHP,el,tot,year}}} \times \left(FCED_{\mathrm{CHP}} + FCED_{\mathrm{GN,CHP,year}}\right) \tag{11}$$

$$FCED_{\mathrm{PV,Al}} = \frac{E_{\mathrm{PV,el,sent,year}}}{E_{\mathrm{PV,el,tot,year}}} \times FCED_{\mathrm{PV}} \tag{12}$$

From Eq. (9), $FCED_{\mathrm{grid}}$, which refers to the Italian electricity mix, is calculated as a function of the electrical energy taken from the grid, while $FCED_{\mathrm{GN}}$, which refers to the Italian gas network, depends on the volume of natural gas taken from the gas network, both during one year of operation. Moreover, from Eq. (10), $FCED_{\mathrm{MES}}$ corresponds to the cradle-to-gate life cycle of the MES. This is calculated by following the procedure of inventory scaling and impact assessment reported in Section 2.2. From Eqs. (11) and (12), the electrical energy sent to the grid is allocated to the users which benefit from this energy [66]. In other words, the impact must be allocated to the users that benefit from the excess of electrical energy from the CHP and PV.

The total cost (TC) is defined as the sum of the amortized investment cost (IC) and the total operational cost (TOC) [11]:

$$TC = IC_{\mathrm{amm}} + TOC \tag{13}$$

where;

$$IC_{\mathrm{amm}} = IC_{\mathrm{MES}} \times \left[\frac{int \times (1+int)^{p}}{(1+int)^{p} - 1}\right] \tag{14}$$

$$TOC = TOC_{\mathrm{fixed}} + TOC_{\mathrm{variable}} + TOC_{\mathrm{fuel}} + TOC_{\mathrm{emission}} + TOC_{\mathrm{grid,el,taken}} - TOC_{\mathrm{grid,el,sent}} \tag{15}$$

The amortized investment cost is calculated by considering an interest rate int of 5.2% and an amortization period p of 10 years.

2.4.2 Operation optimization

At operational optimization level, the optimal operation strategy of the MES components is found by using a DP algorithm. This optimization method is based on the principle of optimality developed by Bellman [32]. The DP algorithm was exploited by the same authors in previous works [34]. In this study, the DP algorithm is nested within the SMO algorithm and the operation optimization problem is therefore simultaneously solved with the design optimization. The DP method requires the representation of the MES model in the state space, where the system is represented by state variables and control variables as follows [32]:

$$x_{\mathrm{k+1}} = y(x_{\mathrm{k}}, u_{\mathrm{k}}) \tag{16}$$

$$E_{\mathrm{k}} = g(x_{\mathrm{k}}, u_{\mathrm{k}}) \tag{17}$$

Equations (16) and (17) describe the state of the plant and its energy production at each time-step of the time horizon.

Equation (16) is a discrete-time dynamic system. The term x denotes the state variables which are used to describe the state of the MES and the term u denotes the decision variables that are used to control the MES components. Finally, Eq. (17) describes the energy production of MES components at each time interval of the time horizon.

Equation (18) defines the cost function of the operation optimization to be minimized [32]:

$$Z(x_0) = \sum_{\mathrm{k=0}}^{\mathrm{N-1}} h_{\mathrm{k}}(x_{\mathrm{k}}, u_{\mathrm{k}}) + h_{\mathrm{N}}(x_{\mathrm{N}}) \tag{18}$$

with h_{k} being the intermediate cost, and h_{N} the final cost. Let the optimal cost function be as follows [32]:

$$Z^{\mathrm{op}}(x_0) = \min_{u \in \mathrm{U}} Z(x_0) \tag{19}$$

where U denotes the space of all admissible control policies. Equation (19) can be rewritten as [32]:

$$Z^{\mathrm{op}}(x_0) = \sum_{\mathrm{k=0}}^{\mathrm{N\text{-}1}} Z_{\mathrm{k}}^{\mathrm{op}} + Z_{\mathrm{N}}^{\mathrm{op}} \tag{20}$$

where;

$$Z_{\mathrm{k}}^{\mathrm{op}} = \min_{u_{\mathrm{k}} \in \mathrm{U_k}} \left\{h_{\mathrm{k}}(x_{\mathrm{k}}, u_{\mathrm{k}}, \mathrm{k}) + Z_{k+1}^{\mathrm{op}}\right\} \tag{21}$$

Equation (21) is called the Bellman equation and represents the principle of optimality. This cost function is solved by dividing the original problem into simple sequences of sub-problems and by moving backward in time. The optimal control policy of the original problem is determined by tracking back the optimal policies which were found for the tail sub-problems. At the end of the recursion, the optimal operation strategy that minimizes the cost function is tracked [32]:

$$u^{\text{op}}=\{u_0^{\text{op}}(x_0),\dots,u_{\text{N}-1}^{\text{op}}(x_{\text{N-1}})\} \tag{22}$$

In this study, the MES state is represented by the TES state of charge, which is updated by taking into account the energy released to the environment [34]:

$$x_{\text{TES,k+1}}=(1-c_{\text{diss}})\times(x_{\text{TES,k}}+E_{\text{TES,th,in,k}}-E_{\text{TES,th,out,k}}) \tag{23}$$

Four decision variables u are used to control the energy production of the CHP, ASHP, AC and TES. The production of the PV and STC generally depends on the renewable energy sources, thus the energy produced by these systems is exploited first. Equations (24) through (32) express the energy production of the energy systems considered in the energy plant [34].

$$E_{\text{STC,th,k}}=G_{\text{k}}\times A_{\text{STC}}\times\eta_{\text{STC,k}}\times\Delta k \tag{24}$$

$$E_{\text{PV,el,k}}=G_{\text{k}}\times A_{\text{PV}}\times\eta_{\text{PV,k}}\times\Delta k \tag{25}$$

$$E_{\text{CHP,th,k}}=u_{\text{CHP,k}}\times P_{\text{CHP,th,nom}}(T_{\text{k}})\times\Delta k \tag{26}$$

$$E_{\text{CHP,el,k}}=\eta_{\text{CHP,el}}(u_{\text{CHP,k}},T_{\text{k}})\times\frac{E_{\text{CHP,th}}(u_{\text{CHP,k}},T_{\text{k}})}{\eta_{\text{CHP,th}}(u_{\text{CHP,k}},T_{\text{k}})} \tag{27}$$

$$E_{\text{ASHP,th/cool,k}}=\begin{cases}u_{\text{ASHP,k}}\times P_{\text{ASHP,th,nom}}(T_{\text{k}})\times\Delta k & \text{In winter}\\ u_{\text{ASHP,k}}\times P_{\text{ASHP,cool,nom}}(T_{\text{k}})\times\Delta k & \text{In summer}\end{cases} \tag{28}$$

$$E_{\text{AC,cool,k}}=u_{\text{AC,k}}\times P_{\text{AC,cool,nom}}\times\Delta k \tag{29}$$

$$E_{\text{TES,th,out,k}}=u_{\text{TES,k}}\times x_{\text{TES,k}} \tag{30}$$

In Eqs. (31) and (32), the GB and CC are used as back-up systems to meet the remaining thermal and cooling energy demands which may not be fulfilled by the other systems.

$$E_{\text{GB,th,k}}=E_{\text{GB,fuel,k}}\times\eta_{\text{GB,k}} \tag{31}$$

$$E_{\text{CC,cool,k}}=E_{\text{CC,el,k}}\times EER_{\text{CC,k}} \tag{32}$$

Finally, the performance of the CHP is corrected according to both load and ambient conditions, while the performance of the ASHP and CC is corrected according to the ambient temperature, as reported in [42].

The operation optimization problem is solved by minimizing the following objective function [26]:

$$OF_{\text{DP}}(x_0)=\alpha\times\left(\frac{PEC(x_0)}{PEC_{\text{CP}}}\right)+\beta\times\left(\frac{OC(x_0)}{OC_{\text{CP}}}\right) \tag{33}$$

At the design optimization level, Eq. (33) is a weighted sum objective function, where the term *PEC* stands for the primary energy consumption, while the term *OC* stands for the operational cost, both normalized to the primary energy consumption and operational costs of a conventional plant. The annual *PEC* is expressed as reported in Eq. (34) [34]:

$$PEC(x_0)=\min_{u\in\text{U}}\sum_{\text{k}=0}^{\text{N-1}}PE_{\text{CHP,k}}(x_{\text{k}},u_{\text{k}})+PE_{\text{GB,k}}(x_{\text{k}},u_{\text{k}})+PE_{\text{grid,el,taken,k}}(x_{\text{k}},u_{\text{k}}) \tag{34}$$

The *PEC* is defined as the sum of the primary energy consumed by the CHP, the GB and the primary energy related to the electrical energy taken from the grid. Moreover, the annual *OC* associated with the operation of the MES is defined as follows [34]:

$$OC(x_0)=OC_{\text{fixed}}+\min_{u\in\text{U}}\sum_{\text{k}=0}^{\text{N-1}}OC_{\text{variable}}(x_{\text{k}},u_{\text{k}})+OC_{\text{fuel}}(x_{\text{k}},u_{\text{k}})+OC_{\text{emission}}(x_{\text{k}},u_{\text{k}})+OC_{\text{grid,el,taken}}(x_{\text{k}},u_{\text{k}})-OC_{\text{grid,el,sent}}(x_{\text{k}},u_{\text{k}})$$
(35)

3. Case study

In this paper, the campus of the University of Parma (Italy) is considered as the case study. The campus is located over an area of about 77 ha and it comprises 21 buildings used for research and educational activities [67]. At present, the plant used to meet the thermal and cooling energy demands on the Campus is composed of GB and CC units, while the electricity demand is provided by the national grid. The goal is to simultaneously determine the optimal design and operational strategy of a MES composed of several energy technologies. The normalized hourly thermal, cooling and electrical energy demands are reported in Fig. 6. The energy demands were normalized with respect to their corresponding peak values for confidentially reasons. The energy demand profiles were both experimentally collected and obtained by means of physical models [68]. For the sake of brevity, environmental data (ambient temperature and solar radiation) are not reported here. However, further information can be found in [67]. Finally, the key nominal technical specifications of the energy technologies considered in this work are reported in Table 2.

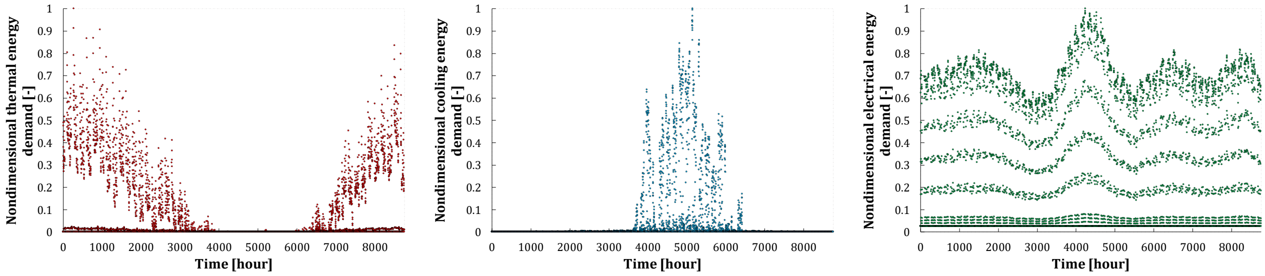

Fig. 6. Nondimensional a) thermal, b) cooling and c) electrical energy demands.

Table 2. Technical specifications of the considered energy systems at nominal conditions.

Technology	Nominal specifications	Lifetime (years)	Reference
STC	η_{STC}=0.8	25	[69]
PV	$\eta_{PV,M}$=0.19; $\eta_{PV,BoS}$=0.9	30	[70, 71]
CHP	$\eta_{CHP,el,nom}=0.251\times P_{CHP,el,nom}^{0.073}$ $P_{CHP,th,nom}=3.027\times P_{CHP,el,nom}^{0.863}$	20	[72]
ASHP	COP=3.2 EER=3.2	20	[73, 74]
GB	$\eta_{GB,th,nom}$=0.93	20	[75]
AC	EER=0.75	20	[76]
CC	EER=3.2	20	[73, 74]
TES	c_{diss}=0.5%	20	[72]

In Fig. 7, the price of electricity of the Italian electricity market in 2019 [77] is reported. As can be seen, the price of electricity changes throughout the year because the market price for electricity is usually determined according to the supply and demand bids of market participants. It should be mentioned that the revenue from selling electricity to the grid [€/MWh] is lower than the electrical energy price by a fixed amount which is specific to the considered country (i.e., 95 €/MWh in Italy).

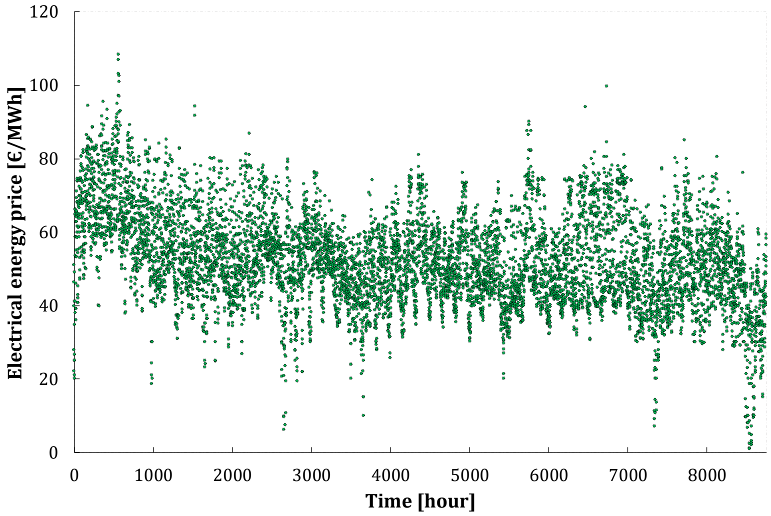

Fig. 7. Hourly profile of the price of electricity [77].

Regarding the Italian gas market, the cost of natural gas for electricity production and heat production in a district heating network is assumed equal to 0.23 €/Stdm^3 [78] (VAT excluded; cost at 2019). Moreover, the cost for CO2 emissions is considered equal to 22 €/tCO_2 [79].

4. Results and discussion

This section presents and discusses the results of the design and operation optimization of the MES. Table 3 summarizes the results in terms of selected technologies and optimal sizes for different combinations of weights α and β. The case (α=1; β=0) corresponds to life cycle energy optimization, while the case (α=0; β=1) corresponds to life cycle cost optimization. For confidentiality reasons, the values of the PV and STC area are normalized with respect to the available area, CHP size is normalized with respect to the electrical peak power of the campus, GB and ASHP sizes are normalized with respect to the thermal peak, and the CC and AC sizes are normalized with respect to the cooling peak. Moreover, the capacity of the TES is expressed in hours by dividing its capacity by the thermal peak power.

From the analysis of Table 3, as the weight of the life cycle energy consumption objective α decreases, the area covered by the PV increases and reaches its maximum if α=0.50 and β=0.50; then it starts decreasing in favor of the STC. If weight α is equal or lower than 0.50, the CHP is selected for cogeneration of thermal and electrical energy. On the other hand, the size of the ASHP decreases as weight α decreases and the option of using a reversible ASHP is discarded when life cycle costs are minimized (α=0; β=1). Since the AC is activated by the thermal energy produced by the STC and recuperated from the CHP, its size is influenced by the STC and CHP sizes. For instance, the size of the AC almost equals the cooling peak power of the campus for the case (α=0; β=1).

Table 3. Optimal design results for the different cases.

Technology	Normalized sizes	α=1; β=0	α=0.75; β=0.25	α=0.5; β=0.5	α=0.25; β=0.75	α=0; β=1
STC	$A/A_{available,tot}$ [-]	0.53	0.35	0.27	0.58	0.82
PV	$A/A_{available,tot}$ [-]	0.47	0.65	0.73	0.42	0.18
CHP [kW$_e$]	$P_{el,nom}/P_{campus,el,peak}$ [-]	0	0	0.52	0.51	0.40
ASHP [kW$_{th}$]	$P_{th,nom}/P_{campus,th,peak}$ [-]	0.35	0.26	0.13	0.01	0
GB [kW$_{th}$]	$P_{th,nom}/P_{campus,th,peak}$ [-]	0.50	0.85	0.62	0.71	0.57
AC [kW$_c$]	$P_{cool,nom}/P_{campus,cool,peak}$ [-]	0.67	0.26	0.61	0.55	0.99
CC [kW$_c$]	$P_{cool,nom}/P_{campus,cool,peak}$ [-]	0.40	0	0.01	0.41	0.01
TES [m^3]	$E_{th,max}/P_{campus,th,peak}$ [h]	2.99	1.23	1.20	0.97	1.52

Figure 8 reports the optimization results in terms of FCED and TEC for the different combinations of weights α and β. The FCED and TEC are normalized with respect to the values of a conventional plant (CP) composed of boilers, chillers and the national grid. By decreasing weight α and increasing weight β, the objective of reducing the TC becomes predominant over the reduction of the FCED. Indeed, compared to the case (α=1, β=0), the case (α=0, β=1) allows the total costs to be reduced by about 37%. However, since the case (α=0, β=1) corresponds to cost optimization, this reduction in total costs leads to an increase in energy consumption of about 47%.

For the cases reported in Table 3, CHP efficiency is 77% for (α=0.50, β=0.50), 73% for (α=0.25, β=0.75) and 70% for (α=0, β=1). Thus, passing from energy consumption optimization to economic optimization, CHP efficiency drops. However, according to the European directives [80], CHP efficiency must be higher than 75%. In Fig. 8, the increase in weight β from 0.25 to 0.5 leads to a drastic drop in life cycle costs. Thus, in order to explore potential solutions between these two cases, an additional optimization case with (α=0.70, β=0.30) is also investigated. Indeed, for this case, CHP efficiency is 82%, which is the highest value among all the other cases. Moreover, this solution is preferable because it provides the best compromise between the FCED and TC, while maintaining CHP efficiency above the minimum threshold. Compared to the case of a CP (composed of boilers, chillers, gas network and electric grid), the case (α=0.70, β=0.30) allows a life cycle energy saving of about 17% and total cost reduction of about 18%.

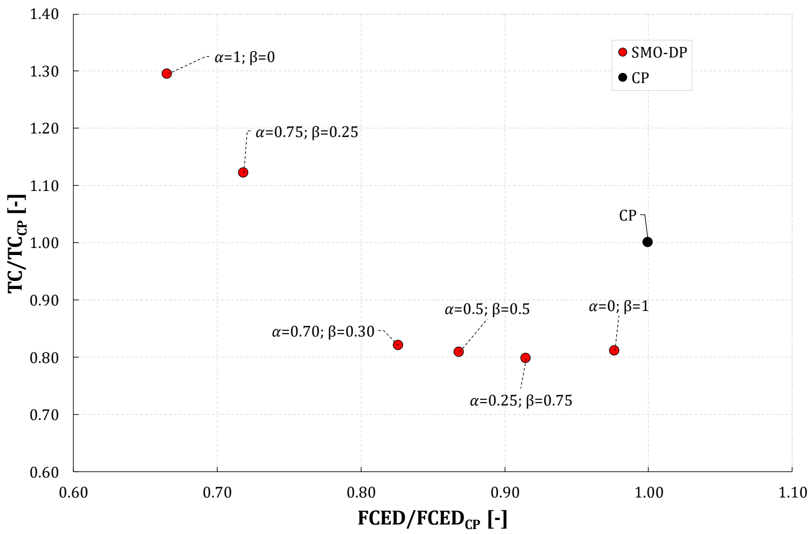

Technology	Normalized sizes	α=0.70; β=0.30
STC	$A/A_{available,tot}$ [-]	0
PV	$A/A_{available,tot}$ [-]	1
CHP [kW$_e$]	$P_{el,nom}/P_{campus,el,peak}$ [-]	0.59
ASHP [kW$_{th}$]	$P_{th,nom}/P_{campus,th,peak}$ [-]	0.23
GB [kW$_{th}$]	$P_{th,nom}/P_{campus,th,peak}$ [-]	0.64
AC [kW$_c$]	$P_{cool,nom}/P_{campus,cool,peak}$ [-]	0.33
CC [kW$_c$]	$P_{cool,nom}/P_{campus,cool,peak}$ [-]	0
TES [m^3]	$E_{th,max}/P_{campus,th,peak}$ [h]	0.54

Fig. 8. Nondimensional FCED and TC for the different cases.

Figure 9 shows how the total FCED is split between the MES, national grid and gas network and how the TC is split between operational and investment costs. From Fig. 9a, the FCED for the MES accounts for its cradle-to-gate life cycle, while the FCED for the grid and the gas network accounts for their cradle-to-gate life cycle including the electricity and gas consumed throughout the useful life of the MES. The CP is considered as a baseline to which the FCED and TC results are compared. From the results, the FCED of the MES is about 10 times higher than the CP, which is mainly due to the higher complexity of the MES which includes several renewable and non-renewable energy systems. Passing from energy optimization (α=1, β=0) to economic optimization (α=0, β=1), the fraction of the FCED related to the gas network becomes much higher, while the fraction related to the grid becomes smaller. This is mainly due to the fact that the option of using ASHP (fed with electricity), which is more favorable in terms of energy consumption, is replaced by the option of using CHP (fed with natural gas), which is economically more favorable (see Fig. 9b). In Fig. 9b, the amortized investment costs of the MES are higher than a CP. However, the operational and running costs of a CP are higher than the ones of the MES. This may be due to the integration of renewable energy systems (i.e., PV and STC), partially renewable systems (i.e., ASHP) and CHP.

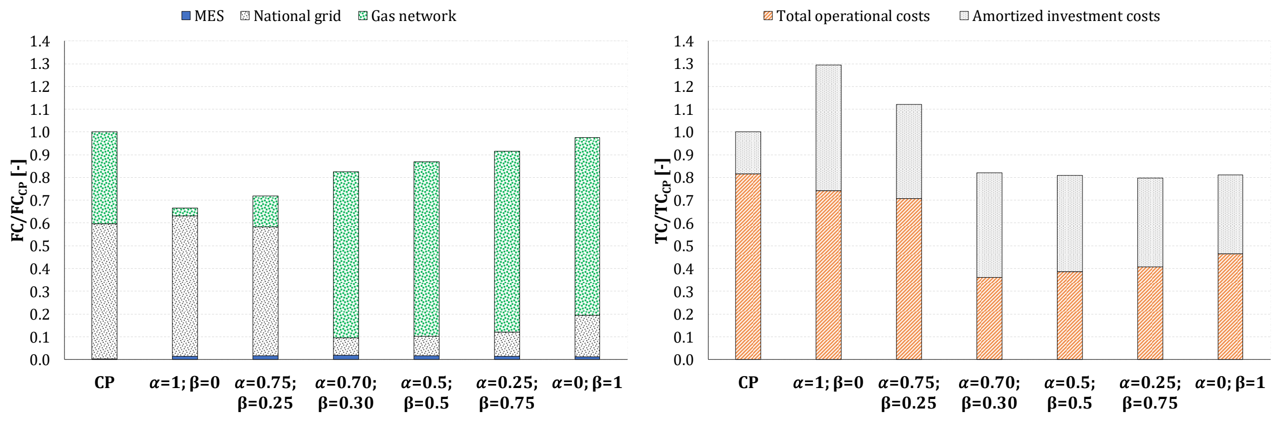

a) b)

Fig. 9. Split of a) FCED and b) TC for the different cases.

Figure 10 shows the contribution of the MES components to the thermal, cooling and electrical energy demands. The thermal energy production is used to meet the thermal demand of the campus and the energy required by the AC. Figure 10a shows that, in order to reduce the life cycle energy demand (α=1, β=0), the thermal demand must be met by STC and ASHP. On the other hand, if the goal is to reduce life cycle costs (α=0, β=1), it is better to meet the thermal demand by means of STC and CHP. The maximum contribution of the CHP is reached for (α=0.7, β=0.3), i.e., where the higher CHP efficiency and best compromise between the two objectives are achieved. Finally, for all cases, the GB supports the energy systems to meet the thermal demand during peak periods.

Since it is reversible, ASHP meets a fraction of the cooling demand. In all cases, the AC is the system that is mostly used for cooling energy production, by exploiting the thermal energy recuperated from the STC and CHP systems. The CC meets a small fraction of the cooling demand (less than 5%) and it is activated when the ASHP is working in heating mode or when the AC is turned off.

In Fig. 10c, the electrical energy demand accounts for the demand of the campus and the electricity required by the heat pump and chiller. For the cases with α>0.7, most of the electrical load is met by the grid, while the remaining part is met by the PV. The fact that the CHP system is not integrated in the MES when α>0.7 may be due to the absence of thermal energy demand during summer. From an energy efficiency point of view, its activation to meet the cooling and electrical demands of the campus does not provide a better option than using heat pumps and taking electricity from the grid. However, this share noticeably changes when the CHP is selected to be included in the MES (α≤0.7). Indeed, when α≤0.7, the CHP meets a high fraction of the electrical energy demand, which reduces the amount of electrical energy taken from the grid. This is mainly due to the high cost associated with the electricity taken from the Italian grid.

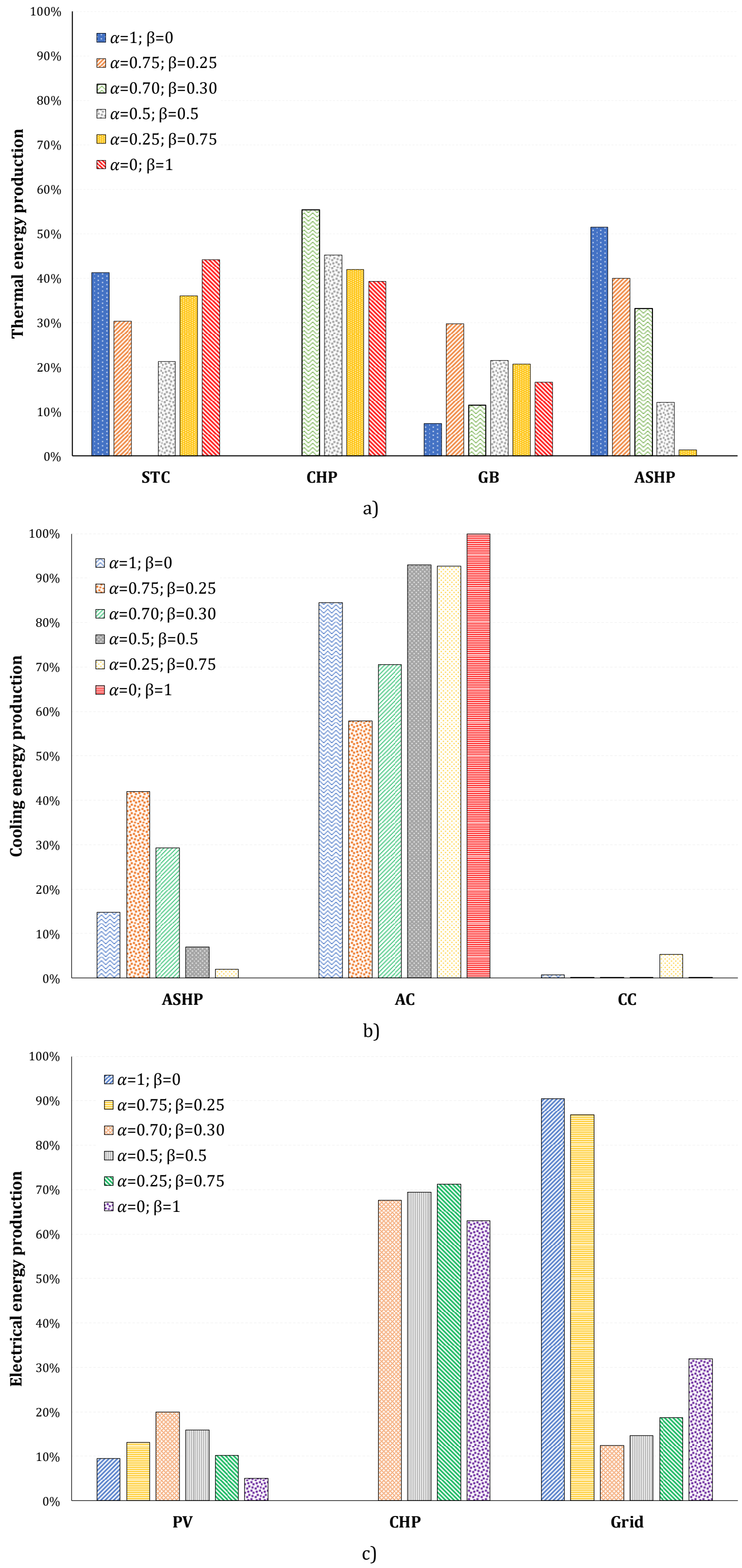

Fig. 10. Annual a) thermal, b) cooling and c) electrical energy contribution of the MES components for the different cases.

In addition to the comparison of the optimization results of the SMO-DP method to the case of a CP (Figs. 8 and 9), the performance of the proposed method is also tested by carrying out a comparison to a particle swarm optimization (PSO) algorithm, which is widely used in the literature for the design optimization of energy systems. In order to perform the simultaneous design and operation optimization of the MES, the PSO is combined with DP. PSO is a population-based optimization algorithm and shares many similarities with evolutionary algorithms, such as the GA. At each iteration of the optimization process PSO generates a number of individuals in the design space; consequently, when DP is combined with PSO, the computational complexity becomes very high. In fact, at each iteration, the operation optimization problem must be solved for each individual of the current population. For this reason, the comparison between the SMO-DP and PSO-DP algorithms is made by considering only the two cases of single objective optimization, i.e., (α=1, β=0) and (α=0, β=1). Table 4 reports the comparison between the two algorithms in terms of energy consumption (for α=1, β=0), total costs (for α=0, β=1) and runtime. The results are normalized with respect to the results of the PSO-DP method. As can be noted, for the case (α=1, β=0), the SMO-DP algorithm estimates a slightly lower energy consumption compared to the PSO-DP method, while for the case (α=0, β=1) the PSO-DP identifies a slightly lower TC (about 2%). However, there is a huge difference in computation time between the two algorithms. The optimizations were carried out on a personal computer with 4 cores and 16 GB RAM. The time taken by the SMO-DP method to solve the simultaneous optimization problem is about 18 hours (i.e., the wall-clock time), while the time taken by the PSO-DP is about 82 hours. Therefore, the adoption of the SMO-DP algorithm allows computation time to be reduced by about 78%. Finally, as clearly highlighted in Table 4, the proposed SMO-DP method allows results to be obtained that are comparable to those obtained by a PSO-DP method with much less effort. This is mainly due to the fact that, unlike the PSO algorithm, the SMO approximates the simulation model by means of a function that is computationally less expensive and converges to the optimal result of the problem with a lower number of iterations.

Table 4. Comparison between the PSO-DP and SMO-DP methods.

	Optimization case	PSO-DP	SMO-DP
FCED [GJ]	(α=1; β=0)	121,880	118,685
TC [k€]	(α=0; β=1)	2,761	2,806
Runtime [hours]		82	18

The surrogate modeling approach achieves a good level of accuracy and at the same time helps to reduce the computational costs. A key limitation of surrogate models is that they may be subject to the so-called *curse of dimensionality*. In general, a higher number of decision variables translates into higher computational complexity for any optimization method [64]. Regarding the surrogate modeling approach, the higher the number of decision variables, the more objective function evaluations (more function evaluations result in more information that can be incorporated into the surrogate model) needed to build an accurate surrogate model [28]. Currently, one way to overcome this limitation is to limit the ranges of the decision variables so that the surrogate model is sufficiently simple to be approximated with a reasonable number of function evaluations. Despite this limitation, the computational results in this paper indicate that the SMO-DP algorithm is a promising algorithm and performs better than commonly used optimization algorithms, such as PSO. The same findings were also discovered by Müller et al. [81], where the surrogate modeling algorithm outperformed other algorithms. Finally, the proposed methodology is general and thus can be applied to other MESs with different energy technologies and to any case study, such as buildings, universities and districts.

5. Conclusions

This paper presented a general methodology for the simultaneous optimization of the design and operation of multi-generation energy systems taking into consideration life cycle energy and economic assessment. The optimal sizes of the system components were determined by using surrogate modeling optimization, while the operation strategy was optimized by means of dynamic programming. Energy systems like the solar thermal collector, photovoltaic panel, combined heat and power, gas boiler, air source heat pump, compression chiller, absorption chiller and thermal energy storage technologies were considered. Life cycle and economic assessments for the investigated systems were carried out by gathering inventory and economic data of commercially available systems of various sizes. The proposed methodology was applied to the campus of the University of Parma (Italy), where a multi-generation energy system was optimally designed and operated by carrying out weighted sum multi-objective optimizations. Moreover, the proposed methodology was able to deal with the dynamics (due to the presence of the storage) and non-linearity associated with the variation in system performance with load and ambient conditions. Unlike other literature studies that use a number of selected days, in this work the simultaneous design and operation optimization was performed by considering one entire year of operation.

The methodology proposed in this paper obtained different solutions based on the weighted sum objectives. The optimization results revealed that the best option from an energy consumption point of view is to use heat pumps and take electricity from the grid. However, if the objective is to reduce the economic costs, the use of cogeneration systems is economically more favorable. Compared to the case of a conventional plant composed of boilers, chillers and the grid, the preferred solution, which reaches the best compromise between energy consumption and economic cost, allowed a life cycle energy saving of about 17% and total cost reduction of about 18%.

Finally, the comparison of the methodology presented in this paper to a methodology based on particle swarm optimization showed that it is possible to obtain comparable results, while reducing the computational time by about 78%.

Acknowledgements

This paper was carried out in the framework of the research program "ENERGYNIUS - ENERGY Networks Integration for Urban Systems (PG/2018/632084)".

References

[1] Rasheed, R., Javed, H., Rizwan, A., Sharif, F., Yasar, A., Tabinda, A.B., Ahmad, S.R., Wang, Y., Su, Y. Life cycle assessment of a cleaner supercritical coal-fired power plant, J. Clean. Prod., 279 (2021), art. no. 123869, DOI: 10.1016/j.jclepro.2020.123869.

[2] Ürge-Vorsatz, D., Cabeza, L.F., Serrano, S., Barreneche, C., Petrichenko, K. Heating and cooling energy trends and drivers in buildings, Renew. Sustain. Energy Rev., 41 (2015), pp. 85-98, DOI: 10.1016/j.rser.2014.08.039.

[3] Mancarella, P. MES (multi-energy systems): An overview of concepts and evaluation models, Energy, 65 (2014), pp. 1-17, DOI: 10.1016/j.energy.2013.10.041.

[4] Mavromatidis, G., Orehounig, K., Bollinger, L.A., Hohmann, M., Marquant, J.F., Miglani, S., Morvaj, B., Murray, P., Waibel, C., Wang, D., Carmeliet, J. Ten questions concerning modeling of distributed multi-energy systems, Build. Environ., 165 (2019), art. no. 106372, DOI: 10.1016/j.buildenv.2019.106372.

[5] Fakhari, I., Peikani, P., Moradi, M., Ahmadi, P. An investigation of optimal values in single and multi-criteria optimizations of a solar boosted innovative tri-generation energy system, J. Clean. Prod., 316 (2021), art. no. 128317, DOI: 10.1016/j.jclepro.2021.128317.

[6] Hassoun, A., Dincer, I. Analysis and performance assessment of a new multigeneration system for net-zero energy houses, Int. J. Energy Res., 40 (2016), pp. 36-50, DOI: 10.1002/er.3272.

[7] Khalid, F., Dincer, I., Rosen, M.A. Thermoeconomic analysis of a solar-biomass integrated multigeneration system for a community, Appl. Therm. Eng., 120 (2017), pp. 645-653, DOI: 10.1016/j.applthermaleng.2017.03.040.

[8] Chitgar, N., Emadi, M.A., Chitsaz, A., Rosen, M.A. Investigation of a novel multigeneration system driven by a SOFC for electricity and fresh water production, Energy Convers. Manag., 196 (2019), pp. 296-310, DOI: 10.1016/j.enconman.2019.06.006.

[9] Mahmood, F., Bicer, Y., Al-Ansari, T. Design and thermodynamic assessment of a solar powered energy–food–water nexus driven multigeneration system, Energy Rep., 7 (2021), pp. 3033-3049, DOI: 10.1016/j.egyr.2021.05.032.

[10] Bahlawan, H., Morini, M., Pinelli, M., Spina, P.R. Dynamic programming based methodology for the optimization of the sizing and operation of hybrid energy plants, Appl. Therm. Eng., 160 (2019), art. no. 113967, DOI: 10.1016/j.applthermaleng.2019.113967.

[11] Lian, J., Zhang, Y., Ma, C., Yang, Y., Chaima, E. A review on recent sizing methodologies of hybrid renewable energy systems, Energy Convers. Manag., 199 (2019), art. no. 112027, DOI: 10.1016/j.enconman.2019.112027.

[12] Fakhari, I., Behzadi, A., Gholamian, E., Ahmadi, P., Arabkoohsar, A. Design and tri-objective optimization of a hybrid efficient energy system for tri-generation, based on PEM fuel cell and MED using syngas as a fuel, J. Clean. Prod., 290 (2021), art. no. 125205, DOI: 10.1016/j.jclepro.2020.125205.

[13] Fakhari, I., Behzadi, A., Gholamian, E., Ahmadi, P., Arabkoohsar, A. Comparative double and integer optimization of low-grade heat recovery from PEM fuel cells employing an organic Rankine cycle with zeotropic mixtures, Energy Convers. Manag., 228 (2021), art. no. 113695, DOI: 10.1016/j.enconman.2020.113695.

[14] Urbanucci, L., Testi, D. Optimal integrated sizing and operation of a CHP system with Monte Carlo risk analysis for long-term uncertainty in energy demands, Energy Convers. Manag., 157 (2018), pp. 307-316, DOI: 10.1016/j.enconman.2017.12.008.

[15] Mahian, O., Javidmehr, M., Kasaeian, A., Mohasseb, S. Optimal sizing and performance assessment of a hybrid combined heat and power system with energy storage for residential buildings, Energy Convers. Manag., 211(2020), art. no. 112751, DOI: 10.1016/j.enconman.2020.112751.

[16] Elkadeem, M.R., Wang, S., Sharshir, S.W., Atia, E.G. Feasibility analysis and techno-economic design of grid-isolated hybrid renewable energy system for electrification of agriculture and irrigation area: A case study in Dongola, Sudan, Energy Convers. Manag., 196 (2019), pp. 1453-1478, DOI: 10.1016/j.enconman.2019.06.085.

[17] Alirahmi, S.M., Dabbagh, S.R., Ahmadi, P., Wongwises, S. Multi-objective design optimization of a multi-generation energy system based on geothermal and solar energy, Energy Convers. Manag., 205 (2020), pp. 112426, DOI: 10.1016/j.enconman.2019.112426.
[18] Vojdani, M., Fakhari, I., Ahmadi, P. A novel triple pressure HRSG integrated with MED/SOFC/GT for cogeneration of electricity and freshwater: Techno-economic-environmental assessment, and multi-objective optimization, Energy Convers. Manag., 233 (2021), art. no. 113876, DOI: 10.1016/j.enconman.2021.113876.
[19] Evins R. Multi-level optimization of building design, energy system sizing and operation, Energy, 90 (2015), pp. 1775-1789, DOI: 10.1016/j.energy.2015.07.007.
[20] Fonseca, J.D., Commenge, J.-M., Camargo, M., Falk, L., Gil, I.D. Multi-criteria optimization for the design and operation of distributed energy systems considering sustainability dimensions, Energy, 214 (2021), art. no. 118989, DOI: 10.1016/j.energy.2020.118989.
[21] Liu, Z., Guo, J., Wu, D., Fan, G., Zhang, S., Yang, X., Ge, H. Two-phase collaborative optimization and operation strategy for a new distributed energy system that combines multi-energy storage for a nearly zero energy community, Energy Convers. Manag., 230 (2021), art. no. 113800, DOI: 10.1016/j.enconman.2020.113800.
[22] Luo, X.J., Oyedele, L.O., Akinade, O.O., Ajayi, A.O. Two-stage capacity optimization approach of multi-energy system considering its optimal operation, Energy and AI, 1 (2020), art. no. 100005, DOI: 10.1016/j.egyai.2020.100005.
[23] Piacentino A., Gallea R., Cardona F., Lo Brano V., Ciulla G., Catrini P. Optimization of trigeneration systems by Mathematical Programming: Influence of plant scheme and boundary conditions. Energy Convers. Manag., 104 (2015), pp. 100-114, DOI: 10.1016/j.enconman.2015.03.082.
[24] Zhang, M., Zhang, N., Guan, D., Ye, P., Song, K., Pan, X., Wang, H., Cheng, M. Optimal design and operation of regional multi-energy systems with high renewable penetration considering reliability constraints, IEEE Access, 8 (2020), pp. 205307-205315, DOI: 10.1109/ACCESS.2020.3036640.
[25] Urbanucci, L., D'Ettore, F., Testi, D. A comprehensive methodology for the integrated optimal sizing and operation of cogeneration systems with thermal energy storage, Energies, 12 (2019), art. no. 875, DOI: 10.3390/en12050875.
[26] Mahmoud P.H.A, Huy P.D., Ramachandaramurthy V.K. A review of the optimal allocation of distributed generation: Objectives, constraints, methods, and algorithms, Renew. Sustain. Energy Rev., 75 (2017), pp. 293-312, DOI: 10.1016/j.rser.2016.10.071.
[27] Abdmouleh Z., Gastli A., Ben-Brahim L., Haouari M., Al-Emadi N.A. Review of optimization techniques applied for the integration of distributed generation from renewable energy sources, Renew. Energy, 113 (2017), pp. 266-280, DOI: 10.1016/j.renene.2017.05.087.
[28] Forrester, A.I.J., Sóbester, A., Keane, A.J. Engineering design via surrogate modelling: A practical guide, John Wiley & Sons Ltd, 2008, ISBN: 978-0-470-06068-1, United Kingdom.
[29] Zhang, W., Liang, Z., Wu, W., Ling, G., Ma, R. Design and optimization of a hybrid battery thermal management system for electric vehicle based on surrogate model, Int. J. Heat Mass Transf., 174 (2021), art. no. 121318, DOI: 10.1016/j.ijheatmasstransfer.2021.121318.
[30] Beykal, B., Boukouvala, F., Floudas, C.A., Pistikopoulos, E.N. Optimal design of energy systems using constrained grey-box multi-objective optimization, Comput. Chem. Eng., 116 (2018), pp. 488-502, DOI: 10.1016/j.compchemeng.2018.02.017.
[31] Perera, A.T.D., Wickramasinghe, P.U., Nik, V.M., Scartezzini, J.-L. Machine learning methods to assist energy system optimization, Appl. Energy, 243 (2019), pp. 191-205, DOI: 10.1016/j.apenergy.2019.03.202.
[32] Bellman R.E. Dynamic Programming. Princeton University Press, 1957.
[33] Chen X.P., Hewitt N., Li Z.T., Wu Q.M., Yuan X., Roskilly T. Dynamic programming for optimal operation of a biofuel micro CHP-HES system, Appl. Energy, 208 (2017), pp. 132-141, DOI: 10.1016/j.apenergy.2017.10.065.
[34] Bahlawan, H., Morini, M., Pinelli, M., Spina, P.R., Venturini, M. Optimization of energy and economic scheduling of a hybrid energy plant by using a dynamic programming approach, Appl. Therm. Eng., 187 (2021), art. no. 116577, DOI: 10.1016/j.applthermaleng.2021.116577.
[35] Facci A.L., Ubertini S. Meta-heuristic optimization for a high-detail smart management of complex energy systems, Energy Convers. Manag., 160 (2018), pp. 341-353, DOI: 10.1016/j.enconman.2018.01.035.
[36] Moradi, H., Esfahanian, M., Abtahi, A., Zilouchian, A. Optimization and energy management of a standalone hybrid microgrid in the presence of battery storage system, Energy, 147 (2018), pp. 226-238, DOI: 10.1016/j.energy.2018.01.016.
[37] Bahlawan, H., Morini, M., Pinelli, M., Poganietz, W.-R., Spina, P.R., Venturini, M. Optimization of a hybrid energy plant by integrating the cumulative energy demand, Appl. Energy, 253 (2019), art. no. 113484, DOI: 10.1016/j.apenergy.2019.113484.
[38] Luo, X.J., Oyedele, L.O., Owolabi, H.A., Bilal, M., Ajayi, A.O., Akinade, O.O. Life cycle assessment approach for renewable multi-energy system: A comprehensive analysis, Energy Convers. Manag., 224 (2020), art. no. 113354, DOI: 10.1016/j.enconman.2020.113354.
[39] Yan, J., Broesicke, O.A., Wang, D., Li, D., Crittenden, J.C. Parametric life cycle assessment for distributed combined cooling, heating and power integrated with solar energy and energy storage, J. Clean. Prod., 250 (2020), art. no. 119483, DOI: 10.1016/j.jclepro.2019.119483.

[40] Mayer, M.J., Szilágyi, A., Gróf, G. Environmental and economic multi-objective optimization of a household level hybrid renewable energy system by genetic algorithm, Appl. Energy, 269 (2020), art. no. 115058, DOI: 10.1016/j.apenergy.2020.115058.
[41] Caduff, M., Huijbregts, M.A.J., Althaus, H.-J., Koehler, A., Hellweg, S. Wind power electricity: The bigger the turbine, the greener the electricity? Environ. Sci. Technol., 46 (9) (2012), pp. 4725-4733, DOI: https://doi.org/10.1021/es204108n.
[42] Barbieri, E.S., Dai, Y.J., Morini, M., Pinelli, M., Spina, P.R., Sun, P., Wang, R.Z. Optimal sizing of a multi-source energy plant for power heat and cooling generation, Appl. Therm. Eng., 71-2 (2014), pp. 736-750, DOI: 10.1016/j.applthermaleng.2013.11.022.
[43] ISO 14040. Environmental Management – Life Cycle Assessment – Principles and Framework; 2006.
[44] ISO 14044: Environmental management – Life Cycle Assessment – Requirements and Guidelines; 2006.
[45] Heck, T. Wärme-Kraft-Kopplung, Ecoinvent Final Report No. 6-XIV, Paul Scherrer Institut Villigen, Swiss Centre for Life Cycle Inventories, Dübendorf, Switzerland, 2007.
[46] Caduff, M., Huijbregts, M.A.J., Koehler, A., Althaus, H.-J., Hellweg, S. Scaling relationships in Life Cycle Assessment: The case of heat production from biomass and heat pumps. J. Ind. Ecol., 18 (3) (2014), pp. 393-406, DOI: https://doi.org/10.1111/jiec.12122.
[47] Bahlawan, H., Morini, M., Spina, P.R., Venturini, M. Inventory scaling, life cycle impact assessment and design optimization of distributed energy plants, Appl. Energy, 304 (2021), art. no. 117701, DOI: 10.1016/j.apenergy.2021.117701.
[48] Wernet, G., Bauer, C., Steubing, B., Reinhard, J., Moreno-Ruiz, E., Weidema, B. The ecoinvent database version 3 (part I): overview and methodology. Int. J. Life Cycle Assess. 21 (2016), pp. 1218–1230, DOI: https://doi.org/10.1007/s11367-016-1087-8.
[49] Wang, J., Yang, Y., Mao, T., Sui, J., Jin, H. Life cycle assessment (LCA) optimization of solar-assisted hybrid CCHP system, Appl. Energy, 146 (2015), pp. 38-52, DOI: 10.1016/j.apenergy.2015.02.056.
[50] Hauschild, M.Z., Huijbregts, M.A.J. Life Cycle Impact Assessment, LCA Compendium – The Complete World of Life Cycle Assessment, 2015, Springer, Dordrecht, DOI: https://doi.org/10.1007/978-94-017-9744-3.
[51] Hischier, R., Weidema, B., Althaus, H.-J., Bauer, C., Doka, G., Dones, R., Frischknecht, R., Hellweg, S., Humbert, S., Jungbluth, N., Köllner, T., Loerincik, Y., Margni, M., Nemecek, T. Implementation of Life Cycle Impact Assessment Methods, Ecoinvent report No. 3, Swiss Centre for Life Cycle Inventories, Dübendorf, Switzerland, 2010.
[52] OpenLCA 1.10.3, GreenDelta. Source: http://www.openlca.org.
[53] Danish Energy Agency. Technology Data - Energy Plants for Electricity and District heating generation. Report 2016. http://www.ens.dk/teknologikatalog.
[54] Henning, H.-M., Döll, J. Solar systems for heating and cooling of buildings, Energy Procedia, 30 (2012), pp. 633-653, DOI: 10.1016/j.egypro.2012.11.073.
[55] Hofmeister, M. and Guddat, M., Techno-economic projections until 2050 for smaller heating and cooling technologies in the residential and tertiary sector in the EU, EUR28861, Publications office of the European Union, Luxembourg, 2017, ISBN 978-92-79-76014-3, doi:10.2760/110433, JRC109034.
[56] Danish Energy Agency. Technology Data - Heating installations. Report 2017. http://www.ens.dk/teknologikatalog.
[57] IRENA (2020), Renewable Power Generation Costs in 2019, International Renewable Energy Agency, Abu Dhabi.
[58] Grosse, R., Christopher, B., Stefan, W., Geyer, R. and Robbi, S., Long term (2050) projections of techno-economic performance of large-scale heating and cooling in the EU, EUR28859, Publications Office of the European Union, Luxembourg, 2017, ISBN 978-92-79-75771-6, doi:10.2760/24422, JRC109006.
[59] Nohlgren, I., Svärd, S.H., Jansson, M., Rodin, J. Electricity from new and future plants, Elforsk, 2014.
[60] European commission directorate-general for energy. Mapping and analyses of the current and future (2020 - 2030) heating/cooling fuel deployment (fossil/renewables), 2016.
[61] Eicker, U., Pietruschka, D. Design and performance of solar powered absorption cooling systems in office buildings, Energy and Buildings, 41 (1) (2009), pp. 81-91, DOI: 10.1016/j.enbuild.2008.07.015.
[62] Regis, R.G., Shoemaker, C.A. A stochastic radial basis function method for the global optimization of expensive functions, Informs J. Computing, 19 (2007), pp. 497-509.
[63] Gutmann, H.M. A radial basis function method for global optimization, Journal of global optimization, 19 (2001), pp. 201-227, https://doi.org/10.1023/A:1011255519438.
[64] Regis, R.G. Stochastic radial basis function algorithms for large-scale optimization involving expensive black-box objective and constraint functions, Comput. Oper. Res., 38-5 (2011), pp. 837-853, DOI: 10.1016/j.cor.2010.09.013.
[65] Powell, M. The theory of radial basis function approximation in 1990, Advances in Numerical Analysis II: Wavelets, Subdivision, and Radial Functions (WA Light, ed.), pp. 105-210.
[66] Frischknecht, R. Allocation in Life Cycle Inventory Analysis for joint production, Int. J. LCA, 5 (2) (2000), pp. 85-95, DOI: http://dx.doi.org/10.1065/lca2000.02.013.
[67] Zatti, M., Gabba, M., Freschini, M., Rossi, M., Gambarotta, A., Morini, M., Martelli, E. k-MILP: A novel clustering approach to select typical and extreme days for multi-energy systems design optimization, Energy, 181 (2019), pp. 1051-1063, DOI: https://doi.org/10.1016/j.energy.2019.05.044.

[68] Zatti, M., Gabba, M., Rossi, M., Morini, M., Gambarotta, A., Martelli, E. Towards the optimal design and operation of multi-energy systems: The “Efficity” project, Environ. Eng. Manag. J., 17 (2018), pp. 2409-2419, DOI: 10.30638/eemj.2018.239.
[69] Fan, J., Chen, Z., Furbo, S., Perers, B., Karlsson, B. Efficiency and lifetime of solar collectors for solar heating plants, Proceedings of the ISES Solar World Congress 2009: Renewable Energy Shaping Our Future.
[70] Jungbluth, N., Stucki, M., Frischknecht, R., Buesser, S. Photovoltaics, Ecoinvent report No. 6-XII, ESU-services Ltd, Uster, Swiss Centre for Life Cycle Inventories, Duebendorf, Switzerland, 2010.
[71] Taylor, N., Jäger-Waldau, A., Photovoltaics Technology Development Report 2020, EUR 30504 EN, Publications Office of the European Union, Luxembourg 2020, ISBN 978-92-76-27274-8, doi:10.2760/827685, JRC123157.
[72] Heck, T. Wärme-Kraft-Kopplung, Ecoinvent Final report No. 6-XIV, Paul Scherrer Institut Villigen, Swiss Centre for Life Cycle Inventories, Dübendorf, Switzerland, 2007.
[73] Heck, T. Wärmepumpen, Ecoinvent Final report No. 6-X, Paul Scherrer Institut Villigen, Swiss Centre for Life Cycle Inventories, Dübendorf, Switzerland, 2007.
[74] Daikin applied systems product catalogue. Link: https://www.daikin.de/content/dam/document-library/catalogues/as/Applied%20Systems_Product%20catalogue_ECPEN17-400_English.pdf.
[75] Jungbluth, N. Erdöl. Ecoinvent report No. 6-IV, Swiss Centre for Life Cycle Inventories, Duebendorf, Switzerland, 2007.
[76] Primas, A. Life Cycle Inventories of new CHP systems, Ecoinvent report No. 20. Swiss Centre for Life Cycle Inventories, B&H AG, Dübendorf and Zurich, 2007.
[77] https://www.mercatoelettrico.org/It/download/DatiStorici.aspx.
[78] https://ec.europa.eu/eurostat/statistics-explained/index.php/Natural_gas_price_statistics.
[79] https://www.minambiente.it/sites/default/files/archivio/allegati/emission_trading/tabella_coefficienti_standard_nazionali_11022019.pdf.
[80] Directive of the European Parliament and of the Council of 25 October 2012. Energy efficiency, amending Directives 2009/125/EC and 2010/30/EU and repealing Directives 2004/8/EC and 2006/32/EC.
[81] Müller, J., Shoemaker, C.A., Piché, R. SO-MI: A surrogate model algorithm for computationally expensive nonlinear mixed-integer black-box global, Comput. Oper. Res., 40-5 (2013), pp. 1383-1400, DOI: 10.1016/j.cor.2012.08.022.

Appendix A. Market analysis and scaling laws of the considered energy systems [47]

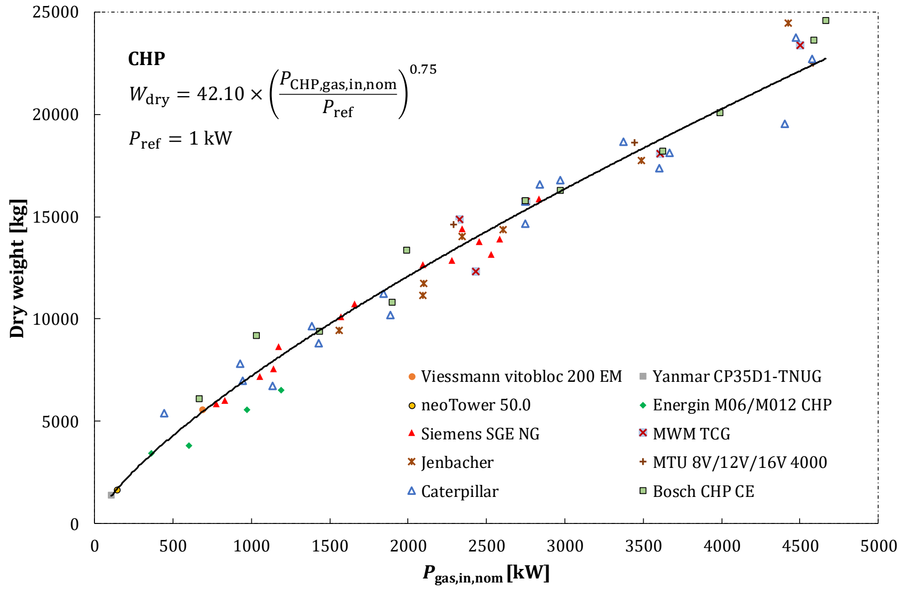

Fig. A1. Dry weight of market available combined heat and power systems as a function of the size.

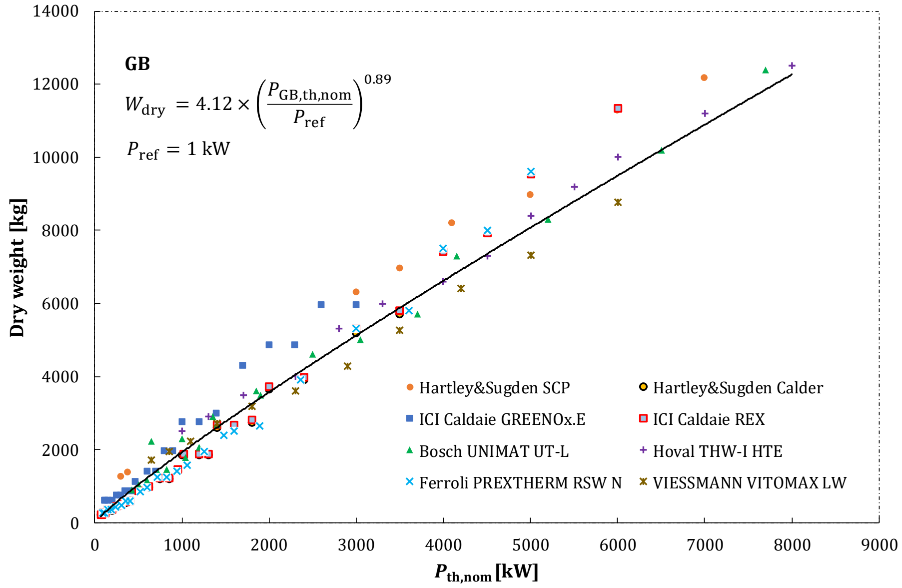

Fig. A2. Dry weight of market available gas boilers as a function of the size.

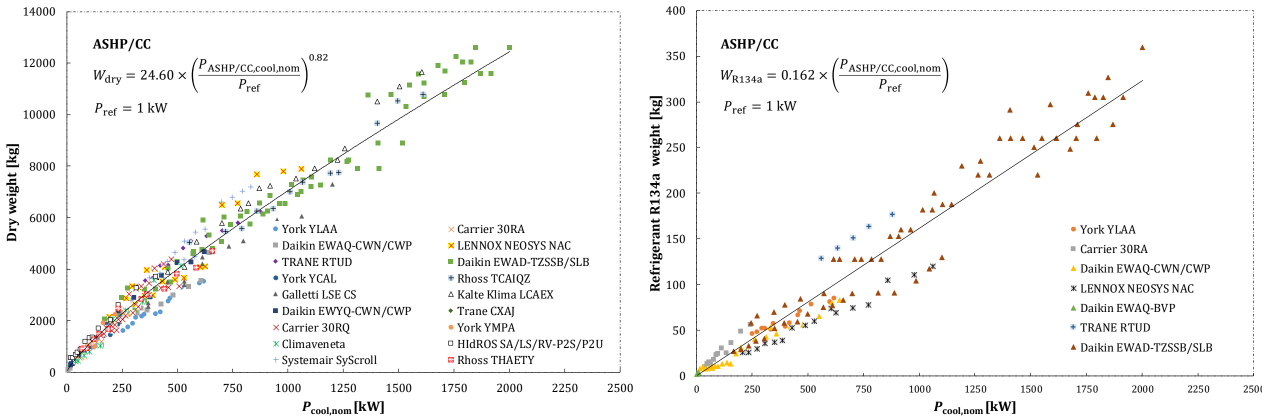

a) Dry weight b) Refrigerant weight

Fig. A3. The a) dry weight and b) refrigerant weight of market available heat pumps/chillers as a function of the size.

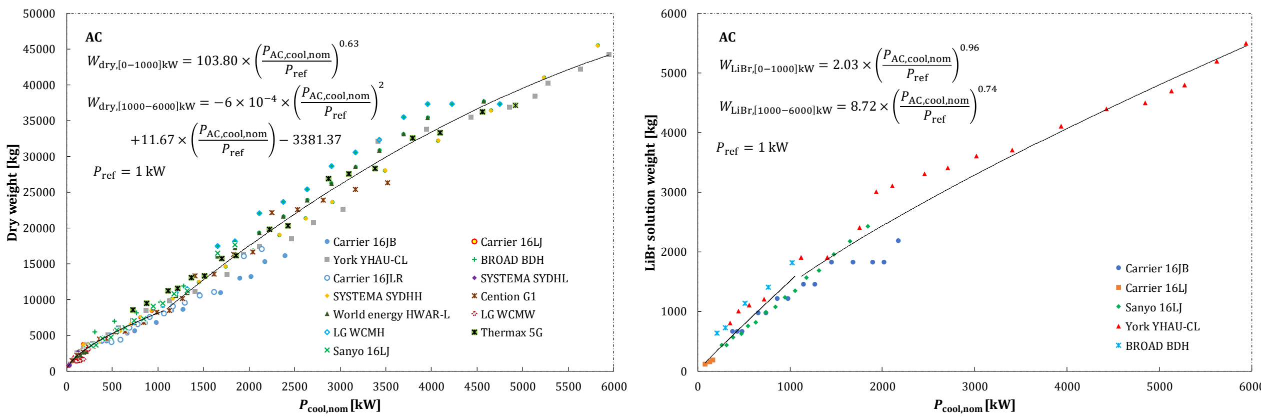

a) Dry weight b) LiBr solution weight

Fig. A4. The a) dry weight and b) LiBr solution weight of market available absorption chillers as a function of the size.

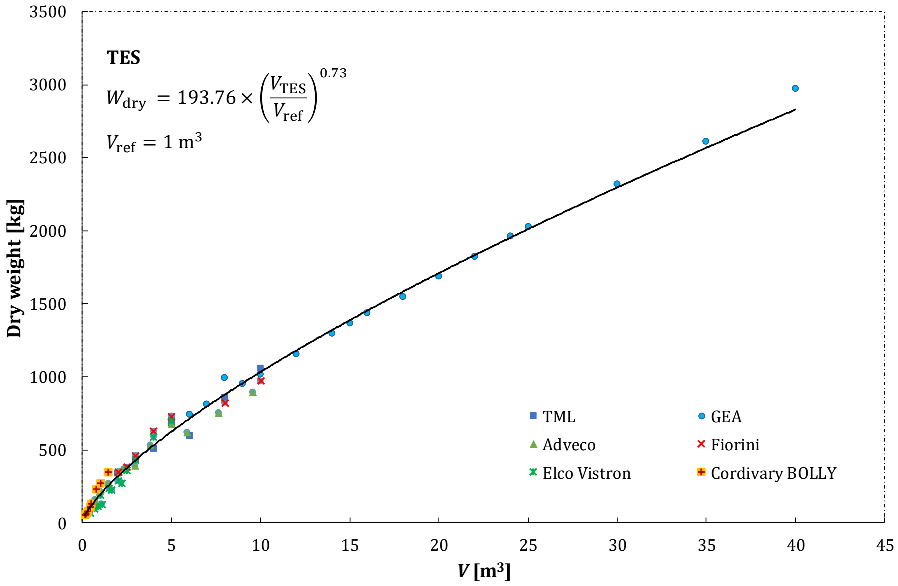

Fig. A5. Dry weight of market available thermal energy storages as a function of the size.